Chemical Physics 89 (1984) 93–102
North-Holland, Amsterdam

PHOTODISSOCIATION OF HYDROGEN PEROXIDE AT 157 nm: ROTATIONAL DISTRIBUTION OF NASCENT OH($^2\Sigma^+$, v', N')

Horst GÖLZENLEUCHTER, Karl-Heinz GERICKE, Franz Josef COMES
Institut für Physikalische und Theoretische Chemie, Robert-Mayer-Strasse 11, D-6000 Frankfurt, FRG

and

Peter F. LINDE
Department of Chemistry, San Francisco State University, 1600 Holloway Avenue, San Francisco, California 94132, USA

Received 22 February 1984

Photodissociation of H_2O_2 at 157 8 nm yields electronically excited OH radicals. The state distribution of nascent fragments, OH($^2\Sigma$, v', N'), has been obtained by spectrally resolved resonance transitions of the OH (A → X) fluorescence. The OH(A) rotational excitation shows a distribution with a maximum at $N' = 21$ with 43% of the total available energy (14040 cm^{-1}) appearing in rotation of the electronically excited fragment. In contrast to rotation, the OH(A) vibrational mode is cold. Only 3% of the OH(A) radicals are in the OH($v' = 1$) state. The fragments are formed statistically between the two spin components of OH($^2\Sigma^+$). The rotational excitation cannot be explained by a simple repulsion of the two fragments. The experimental results strongly suggest that the vibrational OH torsion mode of the parent H_2O_2 is promoted into rotation of the fragments, which is also supported by theoretical arguments. According to these considerations the excess energy is mainly partitioned as rotational energy among the two OH product radicals.

1. Introduction

The photochemistry of small molecules in the gas phase has made remarkable progress in recent years [1]. The development of high-power lasers which emit monochromatic light in the UV and vacuum UV wavelength region has made possible the detection of primary photochemical products under collision-free conditions even in a bulk experiment. A detailed study of the degrees of freedom of the photofragments gives a deep insight into the photodissociation dynamics.

The radiation of electronically excited products can be analyzed in a state-resolved manner. The laser-induced fluorescence or multiphoton ionization are sensitive diagnostics which are well suited for measuring internal degrees of freedom of products and translational energy distribution, if these products are formed in the electronic ground state.

Hydrogen peroxide appears to be an excellent system for the study of the photodissociation dynamics of a tetratomic molecule, because the main photofragments are two OH radicals which can be probed simultaneously by sensitive spectroscopic methods [2]. H_2O_2 exhibits a continuous, almost non-structured absorption spectrum in the UV indicating a short-lived electronic excited state [3]. The dissociation mode is a rupture of the relatively weak O–O bond, resulting in two electronic-ground-state hydroxyl radicals, OH(X $^2\Pi$) [4].

In the vacuum UV one of the two OH fragments can be formed as electronically excited species, thus giving rise to the characteristic OH resonance radiation near 310 nm A $^2\Sigma^+ \rightarrow$ X $^2\Pi$ [5,6]. The partner molecule carries only vibrational, rotational and translational energy, which can be probed by laser-induced fluorescence.

Besides its importance for studying of photodissociation dynamics, hydrogen peroxide is involved in a number of photochemical processes which

0301-0104/84/$03.00

affect the steady concentration of H_2O_2 in the atmosphere. H_2O_2 is mainly produced by recombination of two HO_2 radicals and removed by photodissociation in the UV [7], thus giving rise to the production of the atmospherically important hydroxyl radicals. Its participation in acid rain formation has been claimed [8].

The following paragraphs will discuss the first part of a photodissociation study. The distribution of energy among the different vibrational and rotational states in the electronically excited OH, produced by photodissociating H_2O_2 with the radiation of an excimer laser at 157.8 nm, is observed. The observation of this resonance radiation opens a method to sensitively monitor trace quantities of hydrogen peroxide in the atmosphere.

2. Experimental

The photodissociation of H_2O_2 was carried out with the aid of an excimer laser at the F_2 emission wavelength (157.8 nm). Fig. 1 shows the schematic arrangement of the experiment. The photolyzing laser (EMG 200, Lambda Physik) was operated at 8.5 Hz. The unpolarized and rapidly diverging beam had a rectangular cross section of 30 × 10 mm. With a MgF_2 lens ($f = 300$ mm), it was weakly focused into the reaction cell, which was a cubic aluminum chamber equipped wih a baffled arm to reduce stray light from the MgF_2 entrance window. In order to avoid absorption of the vacuum UV radiation at 157.8 nm by atmospheric O_2 molecules, the 60 cm long path of the light between the laser and the cell was flushed with nitrogen. Laser output energy was 15 mJ per pulse, at a pulse width of 12 ns. The laser showed a decrease in pulse energy to 8 mJ after 10000 pulses, which was the usual laser operation time. For subsequent experiments, the laser was refilled with a fresh F_2/He/Ne mixture. Part of the emission intensity of the laser was monitored to correct for this reduction in power but also to correct for the 20% shot-to-shot fluctuation of the output energy. The intensity of the blue phosphorescence, which occurs when the laser radiation transmits through the MgF_2 window of the cell, was taken as a measure of laser energy. After detection with a photodetector PD (photoelement BPW 34, Siemens), amplification and A/D conversion, this value was read into an Apple II microcomputer.

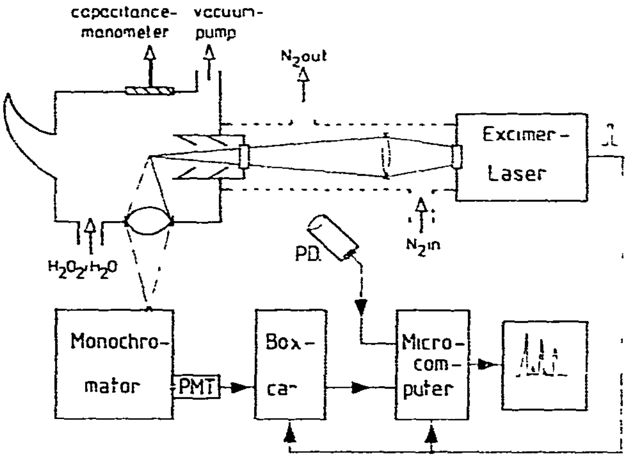

Fig. 1. Schematic diagram of the experimental arrangement. P.D.: Photodetector, PMT: Photomultiplier.

The fluorescence light of the $A\,^2\Sigma^+ \rightarrow X\,^2\Pi$ transitions was observed in a direction perpendicular to the laser beam. A quartz lens was used to focus it on the entrance slit of a 0.5 m grating monochromator (Minuteman, 1200 g/mm, scanning speed 1 Å/min). The spectrally resolved fluorescence light was detected with a photomultiplier (EMI 9635QB) which has a quantum efficiency of $\geqslant 25\%$ in the region between 300 and 420 nm. The multiplier's rise time was 25 ns. To increase the signal, the detector was terminated with 1 MΩ. For time-resolved measurements of total fluorescence, a smaller resistor (50 Ω) was chosen, and the monochromator's slits were fully opened.

The signal was then fed into a boxcar averager (PAR 164) and, after A/D conversion (12 bit), also into the microcomputer which stored the data after each laser pulse. Both instruments were triggered from the laser. This fluorescence signal was divided by the output energy of the excimer laser on a shot-to-shot basis and the final data, which were now normalized to a constant laser output, were monitored on a chart recorder.

H_2O_2 (86% purity) was generously supplied by Degussa. It was stored in a Pyrex glass bottle, mounted under the reaction cell. The vapor was introduced through a glass valve and a short, teflon-coated tubing. Prior to an experiment, it was allowed to flow through the chamber for 1/2 h to passivate the walls. At room temperature, the partial pressure of H_2O_2 vapor is nearly 1/5 of the total pressure of the H_2O_2/H_2O vapor mixture, which was measured with an MKS Baratron capacitance manometer. A vacuum system consisting of a rotary pump and a diffusion pump permitted the total vapor pressure in the cell to be varied from 1 Torr to 1 mTorr. It was kept constant within 5% during the recording of a rotational spectrum of the product. N_2 or Ar could be added for studying rotational relaxation or quenching processes of the excited dissociation products.

3. Results

Irradiation of H_2O_2 in the UV and vacuum UV shows a continuous absorption spectrum. The lowest excited states of the molecule correspond to excitation of O–O antibonding states. Dissociation of the molecule results mainly in a break of the weak O–O bond and formation of two OH radicals in their electronic ground state:

$$H_2O_2 + h\nu \rightarrow OH + OH. \tag{1}$$

At a certain energy one of these OH fragments can be in an electronically excited $OH(A\,^2\Sigma^+)$ state and should emit light when passing back to the ground state. The sum of the energy $D_0 = 17340$ cm^{-1} to form two OH radicals in the electronic ground state $OH(X\,^2\Pi_{3/2})$ and the energy of the lowest electronic excited OH level $T_e = 32440$ cm^{-1} [9] suggest a threshold energy E_d for that behavior of

$$E_d = D_0 + T_e = 49780 \text{ cm}^{-1}, \tag{2}$$

which corresponds to a wavelength of ≈ 210 nm. But in contradiction to this result, even at 184.9 nm, the mercury resonance line, no emission was observed [5].

In a recent study, Suto and Lee [6] reported the quantum yield of the process

$$H_2O_2 + h\nu \rightarrow OH^*(A) + OH(X) \tag{3}$$

with a photolyzing wavelength between 106 and 193 nm. A detectable $OH(A \rightarrow X)$ fluorescence starts to appear at 172.2 nm. At 157.8 nm, the wavelength of the F_2 excimer laser, the actual quantum efficiency for $OH(^2\Sigma^+)$ production is not greater than 0.07, still leaving the production of two ground-state OH radicals as the main dissociation channel.

The present investigations were mainly carried out to measure the nascent rotational-state distribution of the excited radicals formed in the dissociation of H_2O_2. As already mentioned one of the aims of our studies was to find a method to optically detect H_2O_2 in atmospheric environments by simply monitoring the OH fluorescence. Another interest was to obtain a deeper insight into the dissociation dynamics of that molecule. For that reason the fluorescence light from the $OH(^2\Sigma^+, v', N' \rightarrow {}^2\Pi, v'', N'')$ transition was detected with a resolution sufficient to separate the different rotational transitions in the spectrum. From these measurements, we calculated the rotational distribution of the excited OH fragments (fig. 2). Transitions were assigned on the basis of the work of Dieke and Crosswhite [10]. The relative rotational populations $P(N')$ were found from the observed fluorescence intensities of the Q_2 and P_2 branches divided by the corresponding transition probabilities [11] and are plotted versus the rotational quantum number N' of the upper state, F_2. Also from the F_1 spin system several high

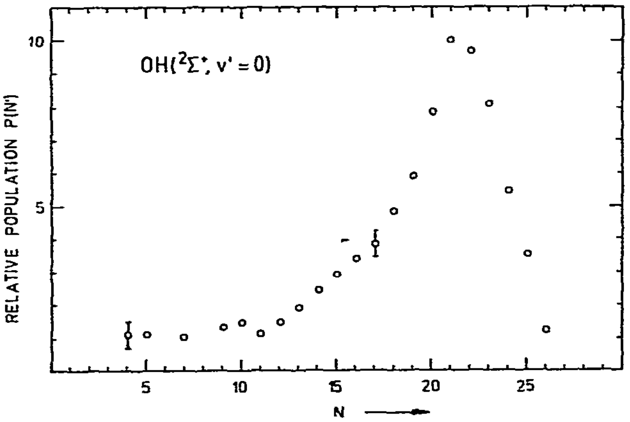

Fig. 2. Relative rotational population of the electronically excited OH fragment in arbitrary units Corrected for predissociation with data from ref. [14].

rotations were observed. This spin system shows a similar distribution among the different rotational states, which means that the rotational energy is partitioned statistically between the two spin systems.

One problem in the study of nascent product distributions in a photodissociative process is the non-radiative energy transfer by collisions between excited- and ground-state molecules (rotational relaxation, quenching). Measurements at 100, 10 and 1 mTorr total vapor pressure of the H_2O_2/H_2O mixture show the same relative intensity distribution in the rotational spectrum, indicating that there is no rotational relaxation in this pressure range.

Quenching cannot be avoided. Lifetime measurements of total fluorescence at 1000, 100, 10 and 1 mTorr agree within 10% with calculated values [12], when H_2O ($k_Q = 13 \pm 2.5 \times 10^6$ $Torr^{-1}s^{-1}$) is assumed to be the main collision partner. However, because only the signal intensity is affected, quenching processes depopulate the excited rotational levels randomly.

To be sure that relaxation was observable in the experiment, the rotational distribution of OH ($A\,^2\Sigma^+, v', N'$) was also determined at very high collision rates with argon and nitrogen as collision partners. N_2 or Ar bubbled through the H_2O_2/H_2O solution at 800 Torr. The analyzed fluorescence spectrum shows that both gases depopulate the higher rotational levels. In addition, nitrogen quenches the integrated signal intensity more than does argon, because the quenching constant of N_2 is ≈ 77 times that of Ar [12].

Final experiments were always performed at total pressures smaller than the pressure at which relaxation phenomena could be detected. All data obtained for the rotational distribution were taken from measurements in the range 1–10 mTorr.

Because predissociation shortens the lifetime (and therefore the fluorescence intensity) of rotational levels with $N' > 23$ in $v' = 0$ [13], populations for these levels are corrected. The true value was determined by multiplying the signal intensity with the factor $1 + \tau_{rad} P_{pred}$ (τ_{rad} is the radiation lifetime, P_{pred} the predissociation probability [14]).

In fig. 3 the natural logarithm of the ratio of rotational population $P(N')$ and degeneration is plotted versus the internal energy $E_{vib} + E_{rot}$ [9]. The distribution is not a Boltzmann distribution and population densities increase between $N' = 10$ and $N' = 21$ (which in principle opens the possibility of a rotational laser).

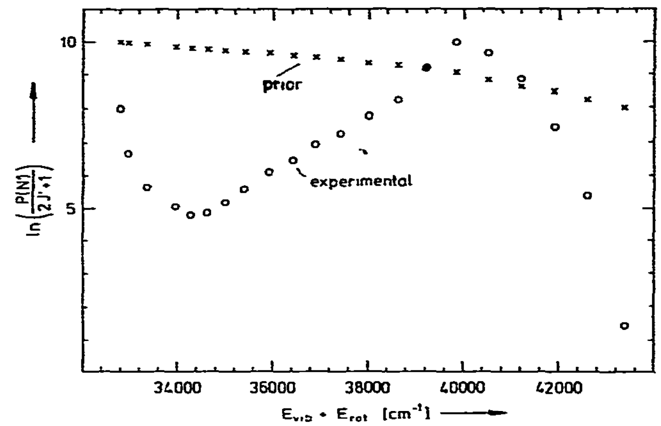

Fig. 3. Boltzmann plot of the experimental rotational distribution of $OH(^2\Sigma^+, v' = 0)$. Also shown is the calculated (strongly deviating) prior distribution for $v' = 0$.

The maximum rotational excitation is centered around $N' = 21$, corresponding to a rotational energy $E_{rot} = 7410\ cm^{-1}$ [9]. The mean rotational energy

$$\langle E_{rot} \rangle = \sum_{N'} P(N') E_{rot}(N') = 6158\ cm^{-1} \qquad (4)$$

corresponds to an OH rotational quantum state of $N' \approx 19$.

Detection of the distribution of photofragments in vibrationally excited $OH(A\,^2\Sigma^+, v' = 1, N')$ states is difficult due to overlapping with transitions from $v' = 0$ states, reduced transition probabilites, and mainly the much lower amount of radicals formed in these levels. The data obtained are insufficient to justify the plot of a rotational distribution for $v' > 0$ states. But we conclude that almost all $OH(A\,^2\Sigma^+)$ are produced in $v' = 0$, and only a very small part ($\leqslant 3\%$) can be found in $v' = 1$. No fragments could be found in $v' = 2$. Thus the dissociation proceeds without vibrational excitation but with extremely high rotational levels.

This result is in good agreement with results obtained at much higher photon energies. Becker et al. [5] have observed $OH(^2\Sigma^+ \rightarrow {}^2\Pi)$ fluorescence at 123 and 147 nm. Although no information on the overall pressure in the experiment is given, their rotational distributions show a very similar structure with the maximum population at $N' = 20$–21. No information on vibrationally excited states were given. It is interesting to notice that the width of the rotational distribution is noticeably larger than in our experiment and that this width increases with the energy of the dissociating radiation. The photolysis of H_2O_2 at 193 and 248 nm produces only ground state fragments [4]. As in the photolysis at 157.8 nm, no vibrational excitation was observed, but the total excess energy was found to be almost exclusively translational energy of the fragments.

4. Discussion

4.1. Energy partitioning

The total excess energy E_{av} which is available to the electronically excited fragment is determined by the initial internal energy $E_{in}(H_2O_2)$ of the parent H_2O_2, the photon energy ($h\nu = 63370\ \mathrm{cm}^{-1}$, $\lambda = 157.8$ Å) and the threshold energy $E_d = 49780$ cm^{-1} [see eq. (2)]:

$$E_{av} = h\nu + E_{in}(H_2O_2) - E_d. \tag{5}$$

H_2O_2 is at thermal equilibrium at room temperature ($T = 300$ K) and has the internal excitation

$$E_{in}(H_2O_2) = E_{vib}(H_2O_2) + E_{rot}(H_2O_2) \approx 450\ \mathrm{cm}^{-1}, \tag{6}$$

where most of the vibrational energy, $E_{vib}(H_2O_2) \approx 120\ \mathrm{cm}^{-1}$, originates from the ν_4 O–H torsion mode (see also table 1.)

Table 1
Normal modes of H_2O_2 vibration [a]

Mode i	Nuclear motion	ω_i'' (cm^{-1}) [b]	f_i
1	O–H symmetric stretch	3600	–
2	OOH symmetric bend	1380	0.45
3	O–O stretch	890	–
4	OH torsion	465	0.46
5	O–H asymmetric stretch	3610	–
6	OOH asymmetric bend	1266	0.45

[a] From ref. [16].
[b] ω_i'' is the energy of the vibrational mode i of the electronic ground state.

The total energy available for excitation of the two OH products is therefore

$$E_{av} = 14040\ \mathrm{cm}^{-1}. \tag{7}$$

The fraction of the available energy partitioned into the various degrees of freedom of OH(A $^2\Sigma^+$) and OH(X $^2\Pi$) is defined in the usual way:

$$f_r(A) = \langle E_r \rangle_A / E_{av}, \quad f_v(A) = \langle E_v \rangle_A / E_{av}, \tag{8}$$

$$f_r(X) = \langle E_r \rangle_X / E_{av}, \quad f_v(X) = \langle E_v \rangle_X / E_{av}, \tag{9}$$

$$f_t(A) = f_t(X) = \tfrac{1}{2}[1 - f_r(A) - f_r(X) - f_v(A) - f_v(X)], \tag{10}$$

where (10) is a consequence of the conservation of energy and linear momentum.

The fraction of internal excitation of the electronically excited OH(A $^2\Sigma^+$) fragment, determined in this experiment is

$$f_r(A) = 43\%, \quad f_v(A) \approx 1\%. \tag{11}$$

Even if the other fragment, OH(X $^2\Pi$), has absolutely no internal excitation the percentage which is released into translation of OH(A $^2\Sigma^+$) is still lower than the percentage of the fraction which is released into rotation:

$$\max. f_t = 28\%. \tag{12}$$

The translational distribution was not directly measured because of the low resolution of the monochromator.

4.2. Surprisal analysis

A reduction of the huge amount of experimental data to a set of few variables and a small number of parameters is quite often obtained by using an information theoretical approach to the fragmentation [15].

The basic, or prior, assumption is that the fragments will be formed in a microcanonical equilibrium, i.e. all quantum states which are energetical accessible will be populated with the same probability P^0. The prior distribution P^0 of the fragments is proportional to the degeneracy of the translation

$$P^0 \propto E_t^{1/2}, \tag{13}$$

where E_t is the translational energy. The prior distribution $P^0(v', N')$ needed to observe OH in the A $^2\Sigma^+$ state is then given by

$$P^0(v', N') \propto (2N'+1) \sum_{N''}^{N''_{\max}} \sum_{v''}^{v''_{\max}} (2N''+1) \times (E_{av} - E_{v''} - E_{N''} - E_{v'} - E_{N'})^{1/2}, \tag{14}$$

where $E_{v''}$ and $E_{v'}$ are the vibrational energies of OH in v'' and v', respectively. E_N stands for the rotational energy of rotational state N. The relatively small difference in energy of the λ and spin doublets in comparison to the rotational energy has not been taken into account.

The prior distribution $P^0(0, N')$ as well as the experimentally observed distribution are shown in fig. 3. As can be seen, the two distributions are quite different. Obviously, the prior distribution does not fit the nascent distribution of OH(A $^2\Sigma^+$, $v' = 0$, N').

The prior distribution

$$P^0(v') = \sum_{N'} P^0(v', N') \tag{15}$$

for the different vibrational levels deviates even more from the experimental findings. According to eq. (15), the relative populations for $v' = 0,1,2,3,4$, and 5 should be 56.07%, 27.48%, 11.66%, 3.93%, 0.84%, and 0.02%, respectively. The experimental findings were 97% for $v' = 0$ and 3% for $v' = 1$. Thus the available energy E_{av} is not distributed equally over the accessible quantum states and the fragmentation must be very specific for the different degrees of freedom.

Quite often the deviation of the prior distribution from the experimental distribution $P_{\exp}(v', N')$ can be described by a linear surprisal I, which is given by

$$I(f) = -\ln\left[P_{\exp}(f)/P^0(f)\right], \tag{16}$$

with $f = E_{rot}/E_{av}$. The surprisal for $v' = 0$ is shown in fig. 4.

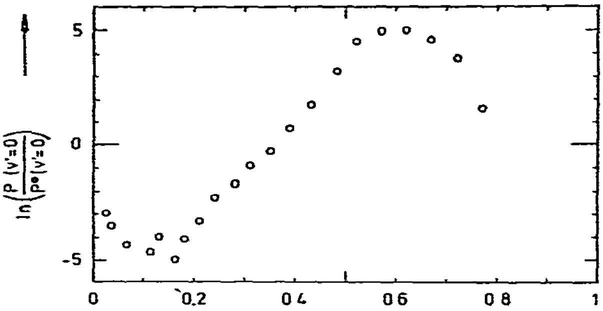

Fig 4 Surprisal plot of the OH($^2\Sigma^+$) population for the dissociation of H_2O_2 at 157.8 nm.

It is obvious that the surprisal is non-linear and the rotational or vibrational distribution cannot be described by two parameters. Only in the limited region between $N' = 10$ and $N' = 21$ can a linear behavior be assumed. But in this region, which only corresponds to a small part of the total produced OH, a Boltzmann plot (fig. 3) can also be characterized by a straight line. Thus a surprisal analysis also indicates a very specific dissociation process.

4.3. Angular momentum

The total angular momentum J_t of the electronically excited $H_2O_2^*$ and of both OH fragments after dissociation is conserved,

$$J_t = J(H_2O_2) + J(h\nu) = J(OH(A)) + J(OH(X)) + L, \tag{17}$$

were $J(H_2O_2)$ is the ground state rotation of H_2O_2, $J(h\nu)$ the contribution of the exciting photon [$J(h\nu) = 1\hbar$], and J(OH(A)) and J(OH(X)) is the rotation of the photofragments in the electronically excited state and in the electronic ground state, respectively. L is the orbital momentum of the HO–OH system and can be calculated classically:

$$L = L_{\max} = \tfrac{1}{2}\mu v s, \tag{18}$$

where μ is the reduced mass of the HO–OH system, s is the impact parameter, and v is the relative velocity of the two fragments. If the translational energy E_t of the fragments is known, this velocity is obtained from

$$v = (2E_t/\mu)^{1/2}. \tag{19}$$

The most probable angular momentum $\bar{J}(H_2O_2)$ of H_2O_2 can be calculated from spectroscopic constants [16] of the parent:

$$\bar{J}(H_2O_2) \approx 10\hbar. \tag{20}$$

Thus a total angular momentum of $\bar{J}_t = 11\hbar$ [see eq. (17)] has to be conserved. Let us now consider the most probable rotation of electronically excited OH which was found to be $\bar{J}(OH(A)) = 21\hbar$ corresponding to a rotational energy of $E_r(\bar{J}) = 7410\ cm^{-1}$. According to eq. (17), this rotation has to be compensated to $J_t = 11\hbar$ by the rotation $J(OH(X))$ of the simultaneously formed ground state OH fragment and by the orbital momentum L.

If we assume that the dissociation starts from a H_2O_2 configuration similar to the ground state (only O–O repulsion), then the angular momentum of the OH(X) is nearly perpendicular to that of OH(A) because of the dihedral angle (see fig. 5). Therefore the OH(X) rotation can compensate for only a small part of $J(OH(A))$.

The orbital momentum L has its maximum when all the remaining energy $E_{rm} = E_{av} - E_r(\bar{J}) = 6630\ cm^{-1}$ is transferred into translation. Eq. (18) gives for L the low value of $L = 1.7\hbar$, if we take for the impact parameter s

$$s = (m_H/m_O + m_H)d_{OH} \approx 0.06\ Å \tag{21}$$

(d_{OH} is the OH bond length in H_2O_2). Thus the basic assumption of a decomposition of H_2O_2 in a configuration similar to the ground state configuration is untenable because the total angular momentum is not conserved.

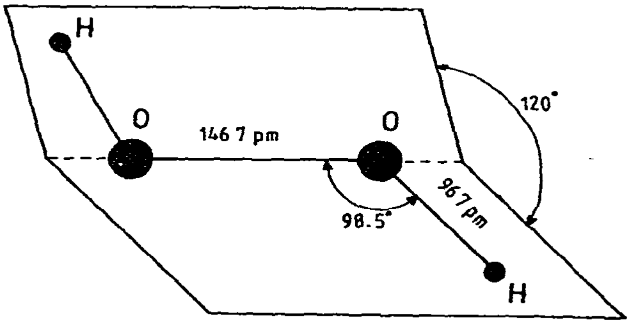

Fig. 5. H_2O_2 ground-state configuration with values taken from ref. [16]

Assuming that the remaining energy E_{rm} is completely transferred into rotation of OH(X), this rotational energy, 6630 cm^{-1}, corresponds to $J(OH(X)) = 18.5$. The necessary relationship

$$\bar{J}(OH(A)) - \bar{J}(OH(X)) \leqslant J_t \approx 11\hbar \tag{22}$$

is fulfilled, but $J(OH(A))$ and $J(OH(X))$ have to point in opposite directions.

4.4. Internal state distribution

4.4.1. Vibration

The Franck–Condon principle explains the observation that the OH photofragment is vibrationally cold. The OH bond length in the parent H_2O_2 molecule is 0.965 Å. In the free OH photoproduct it is nearly the same, $d_{OH} = 1.012$ Å. This implies, similarly to the photodissociation of HONO [17], that the Franck–Condon factors for the decomposition of H_2O_2 to OH($A\ ^2\Sigma^+, v''$) are diagonal, suggesting a fragmentation into vibrationless products.

An impulsive model (see below) predicts essentially no vibrational excitation in the fragments. The HOO angle is close to 90° and any force exerted between the two oxygen atoms has only a small component along the H–O bond axis. Consequently this bond will not be compressed or stretched and practically no vibrational excitation of the OH fragments will occur.

4.4.2. Rotation

The most striking feature in the dissociation of H_2O_2 is the extremely high rotational excitation of the product molecule OH(A). Several possible sources for the fragment rotation have to be considered:

(a) The OH rotation should be related to the ground state rotation of the parent molecule. The rotation of the free radical will mainly originate from the rotation of H_2O_2 around the O–O axis. If this angular velocity of OH in the parent is transferred to the OH fragment, then this mechanism counts to less than 100 cm^{-1} of OH rotational energy. Thus this contribution is far too small to explain the extremely high rotational excitation of the observed fragment.

(b) Another possible explanation for the OH rotation could be an impulse which directs along the central O–O bond during the dissociation process. This impulse will cause a torque on the O atoms in H_2O_2, which can be observed as OH rotation after fragmentation. This model implies a sharp-peaked rotational distribution which cannot be assigned to a temperature-like Boltzmann distribution. If the H_2O_2 configuration in the excited state is similar to that of the ground state, then both fragments, OH(A $^2\Sigma^+$) in the electronically excited state as well as OH in the ground state, should have the same amount of rotation, $J(\mathrm{OH(A)}) = J(\mathrm{OH(X)})$.

This model [18] demands that the OH behaves like a rigid rotator. The H atom would "follow" the torque exerted on the O atom resulting in a rotation of the OH fragment.

We assume that the impulse is directed along the O–O axis. Thus all the available energy, E_{av}, will cause a translation of both O atoms (in opposite directions). The formation of this translation should be independent of the H atoms in the H_2O_2 molecule. This assumption is valid if the dissociation is fast, i.e. the lifetime of the excited parent molecule is less than a rotational period. The translational energy of the O atoms is then partitioned among the different degrees of freedom (translation, rotation, vibration) of the fragments. The rotational energy is obtained if it is assumed that the angular momentum (caused by the velocity of the recoiling O atoms about the center of mass of the OH fragments) is transformed to OH rotation. This rotational energy is given by [18]

$$E_r(\mathrm{OH}) = \left(m_{\mathrm{OH}} r_s \sin^2\delta / 2\theta_{\mathrm{OH}}\right) E_{av}, \tag{23}$$

where δ is the bond angle of HOO in H_2O_2, r_s is the distance of the O atom from the center of mass of the fragment, and θ_{OH} is the moment of inertia of the free radical [19]. Then the rotational energy for electronically excited OH is

$$E_r(\mathrm{OH(A)}) \approx 410\ \mathrm{cm}^{-1}, \quad f_r(\mathrm{A}) \approx 3\%. \tag{24}$$

This energy corresponds to an N' of only ≈ 4. Thus the model fails to predict the high rotational excitation of the fragments, but might explain the rotation of OH in lower rotational states which was also observed in the experiment.

(c) Another source of product rotation is the breaking of a vibrational mode [6] (see table 1) in the excited parent molecule. The H_2O_2 absorption profile is structured. Therefore the lifetime of the electronically excited state is sufficiently long for the development of well-defined vibrational modes which must enter any model calculations. Three possible vibrations exist in H_2O_2 which might be responsible for OH-fragment rotation: the symmetric bending vibration ν_2 (1380 cm^{-1}), the asymmetric bending vibration ν_6 (1266 cm^{-1}), and the OH torsion ν_4 (465 cm^{-1}).

Model calculations [20] have been used to characterize the photodissociation of a triatomic system. We adopt this general model for the H_2O_2 system, but regard one of the terminal hydrogen atoms as part of the neighboring oxygen atom, HO(OH).

For a non-rotating parent the rotational energy $\langle E_r \rangle$ induced by the ν_i vibration is then given by

$$\langle E_r \rangle = f_i \omega_i' \left(v_i' + \tfrac{1}{2} \right), \tag{25}$$

where ω_i' is the energy of the vibrational mode i in the electronically excited state and f_i is the fraction of this vibrational mode which will be transferred into rotation of the fragment. The computed values of f_i are also listed in table 1.

The calculations indicate that each OH radical carries $\approx 45\%$ of that vibrational energy as rotational excitation. From the fluorescence measurements follows that the observed OH(A) radicals contain 43% of the available energy.

All the vibrational modes (ν_2, ν_4, and ν_6) induce an angular momentum of the OH fragments. These momenta are of opposite sign in the case of ν_2 and the sum of the angular momenta of OH(A) and OH(X) is zero. In the case of the ν_4 and ν_6 mode a large value results. From symmetry considerations one would expect that the latter case is less probable because this would have to be counteracted by large orbital angular momenta of the fragments to conserve the total angular momentum [eq. (17)].

In addition we have to consider the internal excitation of the parent molecule H_2O_2 at 300 K. As H_2O_2 is non-linear the molecule has three axes of inertia. The rotation about the O–O axis is the one with the smallest moment of inertia. The other two axes are almost equal. Due to the ratio of nearly 10 for the two different moments of inertia, the rotation about the O–O axis can be considered as only loosely coupled to the two others. The rotation about any axis vertical to the O–O axis which has the largest angular momentum contributes mainly to the orbital angular momentum of the two OH flying apart. If the ν_2 is the promoting mode then the contribution of the H_2O_2 rotation about the O–O axis will cause a small asymmetry of the rotational excitation of the two OH. On the other hand the energy stored in this rotation is very small compared to the observed rotational energy of the fragments. A repulsive force along the O–O axis alone cannot explain the rotational excitation of the OH. The contribution from vibrational modes of the parent molecule seems conclusive. From the above considerations the ν_2 mode is an excellent candidate for the promotive mode.

4.5. Upper electronic state

The interpretation of the experimental findings, rotation of the fragments caused by the excited-OH torsion in the parent, is also supported by ab initio calculations. The basis set used is a double-zeta basis enlarged by polarization and diffuse functions [21].

The ground state of H_2O_2 shows only a minor energy dependence of the dihedral (torsion) angle ϑ. But all excited states, with the exception of the $\sigma\sigma^*$ $^3B_1$ state, show a very strong dependence of the energy (several eV) on the torsion angle.

In the ground state both lone-pair orbitals 4b and 5a are completely occupied. If the 4b orbital has an unpaired electron (^{2}B ion; $n\sigma^*$ ^{3}A, $n\sigma^*$ ^{1}A; Ry ^{3}B, Ry ^{1}B), then a dihedral angle $\vartheta = 180°$ is preferred. On the other hand, if the 5a orbital has an odd electron (^{2}A ion; $n\sigma^*$ ^{3}B, $n\sigma^*$ ^{1}B; Ry ^{3}A, Ry ^{1}A), then the torsion angle will be $\vartheta = 0°$. Thus the energy of the 4b orbital decreases with decreasing ϑ, while with increasing torsion angle the energy of the 5a orbital decreases.

At 157.8 nm only two different excited states of H_2O_2 can be produced. These are the $n\sigma^*$ ^{1}A or the $n\sigma^*$ ^{3}B states, which can dissociate to $OH(^2\Pi) + OH(^2\Sigma^+)$. From purely qualitative considerations it cannot be decided which of these is responsible for the fragmentation. However, the ^{1}A $n\sigma^*$ $4b^1$ $5b^1$ state has a much lower energy at $\vartheta = 180°$ than at the angle of the equilibrium configuration, while the energy of the ^{3}B $n\sigma^*$ $5a^1$ $5b^1$ state shows a strong gradient to $\vartheta = 0°$.

Thus both states can induce a high rotational excitation of the fragments either by increasing (^{1}A state) or by decreasing (^{3}B state) the torsion angle ϑ. As a consequence the rotations of the two OH fragments should have opposite direction.

Acknowledgement

This work has been performed as part of the program of the “Sonderforschungsbereich 73”. HG is grateful to the Deutsche Forschungsgemeinschaft for a personal support. PFL. thanks the Gmelin-Institut for release time to participate in this research. The authors thank E.A. Reinsch for many helpful discussions. Especially the contribution from V. Staemmler on the excited states is gratefully acknowledged.

References

[1] H. Okabe, in: Photochemistry of polyatomic molecules (Wiley, New York, 1976) p. 282

[2] N.R. Greiner, J Chem. Phys 47 (1967) 4373.

[3] M. Schürgers and K.H. Welge, J. Chem. Phys. 51 (1969) 4678

[4] A. Jacobs, K. Kleinermanns, H. Kluge and J. Wolfrum, J. Chem Phys. 79 (1983) 3162;
G. Ondrey, N. van Veen and R. Behrson, J. Chem. Phys. 78 (1983) 3732;
E.M. Evleth, J. Am. Chem. Soc. 98 (1976) 1637.

[5] K.H. Becker, W. Groth and D. Kley, Z. Naturforsch. 20a (1965) 748.

[6] M. Suto and L.C. Lee, Chem Phys. Letters 98 (1983) 153.

[7] J. Heicklen, in: Atmospheric chemistry (Academic Press, New York, 1976) p. 89;
P.J. Crutzen and J. Fishman, Geophys Res. Letters 4 (1977) 321.

[8] S.A Penkett, B.M.R. Jones, K.A. Brice and A E.J. Eggleton, Atmos. Environ. 13 (1979) 123;
L.R. Martin and D.E. Damschen, Atmos. Environ. 15 (1981) 1615.

[9] M. Nuss, K.-H. Gericke and F.J. Comes, J. Quant. Spectry. Radiative Transfer 27 (1982) 191.

[10] G.H. Dieke and H.M. Crosswhite, J. Quant. Spectry. Radiative Transfer 2 (1961) 97.

[11] W.L. Dimpfl and J.K. Kinsey, J. Quant. Spectry. Radiative Transfer 21 (1979) 233.

[12] K.R. German, J. Chem. Phys. 62 (1975) 2584;
P.M. Selzer and C.C. Wang, J. Chem. Phys. 71 (1979) 3786.
[13] J. Brzozowski, P. Erman and M. Lyyra, Physica Scripta 17 (1978) 507.
[14] R.A. Sutherland and R.A. Anderson, J. Chem. Phys. 58 (1973) 1226.
[15] R.D. Levine and R.B. Bernstein, in: Molecular reaction dynamics (Oxford Univ. Press, London, 1974) p. 137.
[16] P.A. Giguère and T.K.K. Srinivasan, J. Mol Spectry. 66 (1977) 168;
O. Brain and P.A. Giguere, Can. J. Chem. 33 (1955) 527;
P.A. Giguère, J. Chem Phys 18 (1950) 88.
[17] R. Vasudev, R.N. Zare and R.N. Dixon, Chem. Phys. Letters 96 (1983) 399.
[18] A.F. Tuck, J. Chem. Soc. Faraday Trans. 2 (1977) 689.
[19] K.P. Huber and G. Herzberg, Constants of diatomic molecules (Van Nostrand, Princeton, 1979).
[20] M D. Morse and K.F. Freed, J. Chem Phys. 78 (1983) 6045;
M D. Morse, Y.B. Band and K.F. Freed, J. Chem. Phys. 78 (1983) 6066.
[21] V. Staemmler, private communication.